

## Article

# Influence of Basicity and Calcium-Containing Substances on the Consolidation Mechanism of Fluxed Iron Ore Pellets

Kuo Liu, Feng Chen , Yufeng Guo , Yajing Liu, Shuai Wang  and Lingzhi Yang

School of Minerals Processing and Bioengineering, Central South University, Changsha 410083, China; liukuo@csu.edu.cn (K.L.); 195611027@csu.edu.cn (Y.L.); wang\_shuai@csu.edu.cn (S.W.); yanglingzhi@csu.edu.cn (L.Y.)

\* Correspondence: csuchenf@csu.edu.cn (F.C.); yfguo@csu.edu.cn (Y.G.)

**Abstract:** The application of fluxed pellets in iron making industry has attracted considerable attention because of the better metallurgical properties than acid pellets and environmental friendliness compared to sinters. However, fluxed pellets with different binary basicity ( $\text{CaO}/\text{SiO}_2$ ) exhibited significant differences in phase composition, microstructure and consolidation mechanism. These differences mainly stemmed from the influence of calcium-containing substances in fluxed pellets. Herein, the theoretical investigation discovered the calcium-containing substances from fluxed pellets, including calcium iron silicate, calcium silicate and complex calcium ferrite (SFCA), which determined the properties of fluxed pellets. Microstructure analysis revealed that the calcium-containing substances filled between hematite particles were used as a binding phase to assist in pellets' consolidation. Furthermore, the calcium-containing binding phase formed in the low-basicity (0.4–1.0) pellets was mainly composed of the calcium iron silicate glassy phase, while the binding phase of the high-basicity (1.0–1.2) pellets was dominated by SFCA belonging to  $\text{SiO}_2\text{-Fe}_2\text{O}_3\text{-CaO-Al}_2\text{O}_3$  multivariate system. In comparison, SFCA exhibited better crystallinity and reducibility than calcium iron silicate. Within the roasting temperature range of 1200–1250 °C, the increase of basicity contributed to the fluxed pellets obtaining better strength. To sum up, fluxed pellets with SFCA as the main calcium-containing binding phase can be obtained by increasing the basicity above 1.0–1.2, which was imperative for further improving the physical and metallurgical properties of fluxed pellets.

**Keywords:** fluxed pellets; basicity; calcium; consolidation mechanism; SFCA



**Citation:** Liu, K.; Chen, F.; Guo, Y.; Liu, Y.; Wang, S.; Yang, L. Influence of Basicity and Calcium-Containing Substances on the Consolidation Mechanism of Fluxed Iron Ore Pellets. *Metals* **2022**, *12*, 1057. <https://doi.org/10.3390/met12061057>

Academic Editors: Rajesh Kumar Jyothi, Rafael Santos, Shivakumar Angadi and Sanjay Agarwal

Received: 19 May 2022

Accepted: 14 June 2022

Published: 20 June 2022

**Publisher's Note:** MDPI stays neutral with regard to jurisdictional claims in published maps and institutional affiliations.



**Copyright:** © 2022 by the authors. Licensee MDPI, Basel, Switzerland. This article is an open access article distributed under the terms and conditions of the Creative Commons Attribution (CC BY) license (<https://creativecommons.org/licenses/by/4.0/>).

## 1. Introduction

High-grade lump ores, sinters and pellets are the main furnace burden used to produce pig iron in iron and steel companies. Compared with lump ores and sinters, pellets are considered to have a higher iron grade, uniform particle size and lower coke consumption [1]. The negative impacts of traditional furnace burden on energy resource consumption and environmental pollution concerns have been increasing in recent decades, which stimulated extensive efforts to develop fluxed pellets with better quality and metallurgical properties to replace parts of the sinters and lump ores [2,3]. Up to now, the role of fluxed pellets has received ever-increasing attention in metallurgical research. Fluxed pellets not only demonstrate better consolidation strength and metallurgical performance but also enhance furnace slag formation [4]. More importantly, attributed to the high binary basicity ( $\text{CaO}/\text{SiO}_2$ ), fluxed pellets can replace sinters in large quantities as ironmaking charge, which is helpful to improve the environmental pollution and reduce the amount of coke usage [5].

In industrial production, the basicity of pellets is adjusted by adding limestone, dolomite and other calcium-containing raw materials. The change in basicity can give rise to a significant discrepancy in the physical and metallurgical properties of fluxed pellets [6].

Several studies have documented that the appropriate basicity can usually make the fluxed pellets have sufficient consolidation strength [7]. Increasing the consolidation strength of fluxed pellets contributes to reducing internal stress so as to avoid the disintegration and abnormal swelling, improve the permeability of furnace burden and ensure the uniform distribution of airflow in a furnace [8]. Nevertheless, fluxed pellets with basicity below 0.8 will produce severe reduction disintegration and abnormal swelling during iron making. As the basicity continues to increase, the above metallurgical properties can be improved [9]. At present, the research about the metallurgical properties of fluxed pellets usually focuses on the effect of iron oxide crystal structure transformation during the reduction process [10] but ignores the influence of calcium-containing substances. In fact, the phase composition and consolidation mechanism of calcium fluxed pellet with different basicity are closely related to its metallurgical properties [11].

According to previous studies, the consolidation of fluxed pellets included solid-phase consolidation and liquid-phase bonding [12,13]. Solid phase consolidation relies on microcrystalline junctions formed by particle diffusion between adjacent hematite grains to provide strength, which is mainly affected by roasting temperature and oxidizing atmosphere [14,15]. Liquid phase bonding requires that the roasting temperature reaches the melting temperature of low-melting-point compounds. When satisfying the temperature conditions, these compounds can be converted into a liquid phase to adhere to hematite particles and eventually form a high-strength microstructure after cooling and crystallization [16]. Our studies found that there are significant variations in the type and composition of the calcium-containing binding phase as the basicity of fluxed pellets varied [17]. This is the main reason for the differences in physical and metallurgical properties of fluxed pellets with different basicity [18,19].

From what has been discussed above, the research on the consolidation mechanism of fluxed pellets is helpful to improve their physical and metallurgical properties. Up to now, the effect of basicity and calcium-containing substances on the consolidation mechanism of fluxed pellets has not reached a unified conclusion. In particular, the formation conditions, phase composition and microstructure characteristics of calcium-containing substances need to be further investigated. Given this, exploring the influence of basicity and calcium-containing substances on fluxed pellets preparation is imperative for further improving the performance index of ironmaking furnace burden. Herein, TG/DSC synchronous thermal analysis, X-ray diffraction analysis, optical microscope image analysis, SEM-EDS and EPMA technology were used to study phase composition, formation temperature of liquid phase, microstructure and consolidation mechanism of fluxed pellets in different basicity ranges. The results of these studies would provide technical support and a theoretical basis for preparing fluxed pellets with the appropriate basicity and calcium-containing substances composition to further improve the physical and metallurgical performance of pellets.

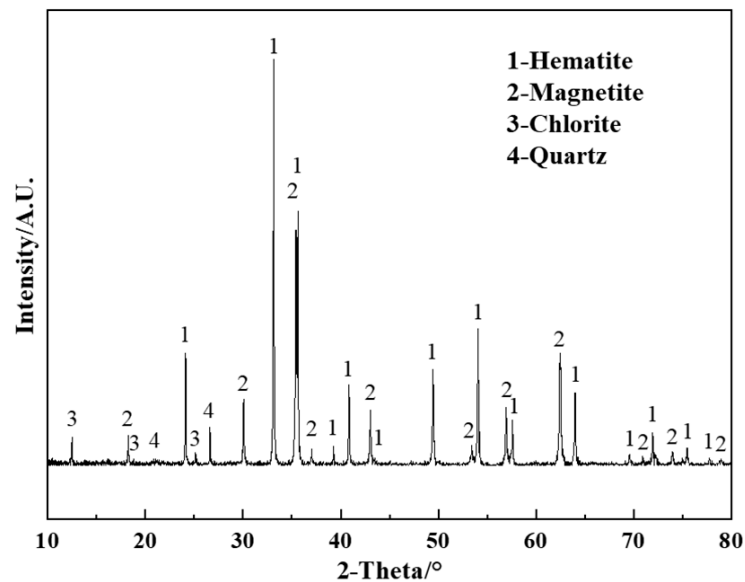
## 2. Experimental

### 2.1. Materials

In this study, iron concentrate, bentonite and limestone used to prepare fluxed pellets were taken from an iron and steel corporation in China. The chemical composition of the above materials is listed in Table 1. Bentonite contained 58.25 wt% montmorillonite was used as a binder to improve the strength of green pellets. Limestone as a flux agent would not introduce more impurity elements to raw materials. The X-ray diffraction (XRD) spectrum of iron concentrate was shown in Figure 1, which indicated that the main phase composition of iron-bearing minerals was hematite, followed by magnetite. The presence of magnetite was conducive to reducing energy consumption and improving the strength of solid-phase consolidation. Moreover, a small amount of silicone-containing gangue, including quartz and chlorite, existed in iron concentrate.

**Table 1.** Chemical compositions of the materials (wt%).

Raw Material	TFe	FeO	CaO	SiO <sub>2</sub>	MgO	Al <sub>2</sub> O <sub>3</sub>	K <sub>2</sub> O	Na <sub>2</sub> O	S	P	LOI
Iron concentrates	66.23	10.52	0.36	3.42	0.48	0.73	0.053	0.077	0.048	0.026	1.02
bentonite	3.06	-	4.55	60.14	2.88	9.10	0.93	2.08	0.031	0.049	10.25
limestone	0.36	-	54.53	1.06	0.53	0.44	0.14	0.037	0.018	0.0084	42.68

**Figure 1.** XRD pattern of iron concentrate.

## 2.2. Experimental Method

### 2.2.1. Pelletizing

The iron concentrate was mixed with bentonite and limestone according to different basicity (CaO/SiO<sub>2</sub>). The mass percentage of bentonite in the mixture was guaranteed to be constant at 1.2%. Then, raw materials were wet with the appropriate amount of water to maintain the same moisture at 9% in each pelletizing test. The raw materials were mixed repeatedly to ensure that the limestone completely dispersed in the iron concentrate. The pelletizing test was carried out in a disc pelletizing machine. Fluxed green pellets of a similar size were prepared within 12 min and sieved out with a diameter of 12–14 mm. Then, the green pellets were dried for subsequent preheating and roasting tests.

### 2.2.2. Preparation of Oxidized Roasting Pellets

The preheating and roasting test was carried out in a horizontal tube furnace. As shown in Figure 2, the front region of the tube furnace simulated the preheating process, and the rear region simulated the oxidizing roasting process. According to the pre-established preheating and roasting conditions in Figure 3, green pellets were placed in a porcelain boat and pushed into the preheating region (1070 °C) through five heating stages. After 8 min of preheating, the porcelain boat with preheating pellets was pushed into the roasting region and kept warm for 10 min. Subsequently, the roasted pellets were dragged back to the original preheating region for cooling. After 5 min, the roasted pellets were removed from the furnace. It was worth noting that we conducted optimization experiments on the preheating and roasting thermal regulation earlier. Herein, in order to accurately study the effect of basicity on the consolidation mechanism of fluxed pellets, we chose fixed preheating (1070 °C) and roasting (1230 °C) thermal regulation for subsequent XRD, SEM and EPMA analysis.

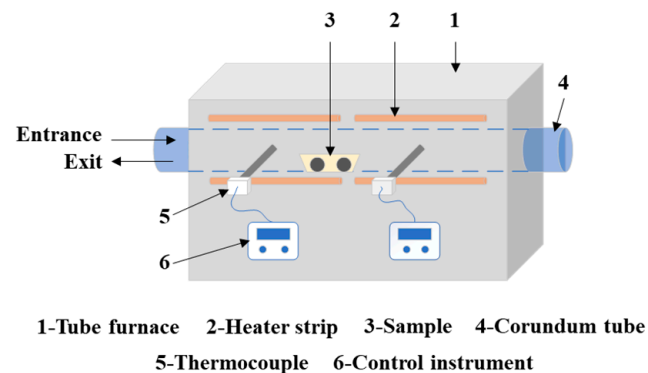


Figure 2. Schematic diagram of roasting apparatus.

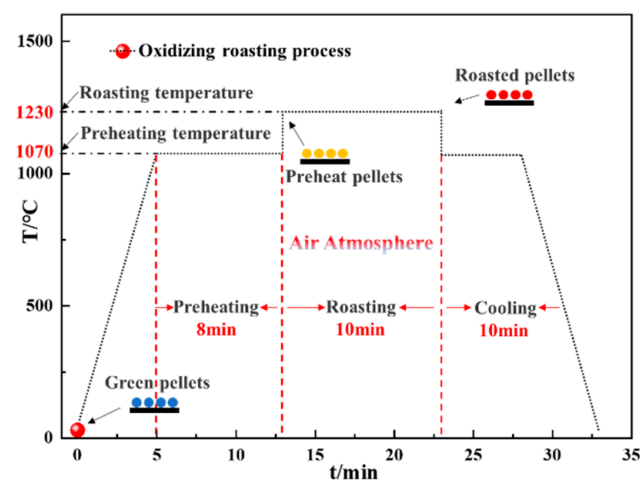
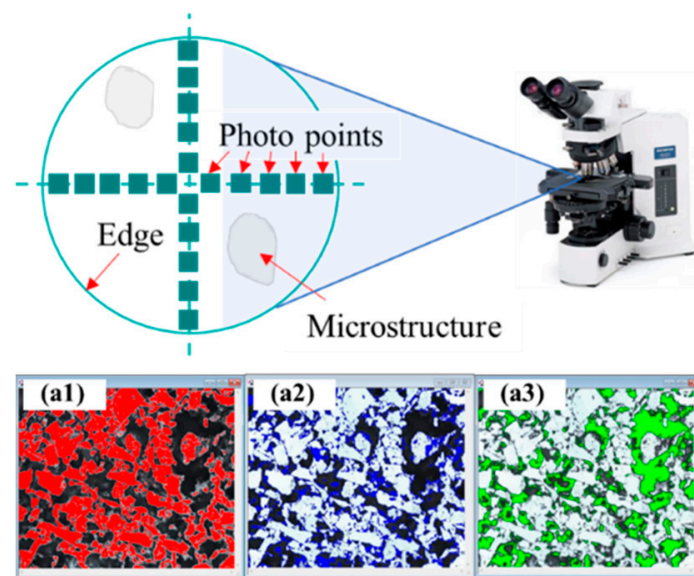


Figure 3. Flow chart of roasting pellets preparation.

### 2.2.3. Analysis and Characterization

The compressive strength of roasted pellets was tested according to ISO 4700-2015 standard. The thermal gravimetric and differential scanning calorimetry (TG/DSC) analysis of the pelletizing mixture was performed using a synchronous thermal analyzer (TG/DSC, NETZSCH STA 449C, Selb, Germany) at the temperature range of 35 °C to 1350 °C with a heating rate of 10 K/min in air atmosphere. The phase composition of the oxidized roasted pellets with different basicity was determined with an X-ray diffraction spectrometer (XRD, Empyrean, Malvern PANalytical, Egham, UK). The microstructures and compositions of roasted pellets were determined using a field emission electron scanning electron microscope (SEM, TESCAN MIRA3, TESCAN, Brno, Czech Republic) equipped with an EDAX energy dispersive X-ray spectrometer (EDS, Oxford X-max 20, Oxford Instruments, Oxford, UK). The element distribution of the binding phase in fluxed pellets was characterized using an electron probe microanalysis (EPMA, EPMA-1720H, Shimadzu Co., Ltd., Kyoto, Japan).

Image-pro Plus 6.0 software was used to analyze micrographs of fluxed pellets. As shown in Figure 4, a set number of micrographs on the X-axis and Y-axis of each different basicity pellets cross-section taken by the optical microscope were selected. Based on the difference in color, gray and brightness, image-pro Plus 6.0 could be used to demarcate and calculate the area percentage of each phase (red—hematite, blue—binding phase and green—pore) in the optical micrograph. This analysis method mainly described the variation trend of hematite crystal, binding phase and pore content.



**Figure 4.** Schematic diagram of optical micrograph statistical analysis ((a1) Red-hematite, (a2) Blue-binding phase, (a3) Green-pore).

### 3. Results and Discussion

We studied the composition of calcium-containing substances in fluxed pellets with different basicity. Subsequently, the consolidation mechanism of different basicity pellets was summarized according to the microstructure and distribution of these calcium-containing substances. Based on these results, we analyzed the reaction during roasting and the influence of basicity on the consolidation strength.

#### 3.1. Phase Composition of Fluxed Pellets with Different Basicity

To investigate the consolidation mechanism of fluxed pellets, the XRD method was used to analyze the phase composition of pellets with 0.2–1.2 basicity. From the diffraction results in Figure 5, the phase composition of fluxed pellets changed with the basicity. The natural-basicity (0.2) pellets were composed of hematite and quartz. With the addition of limestone, calcium iron silicate and complex calcium ferrite (SFCA) began to appear in pellets. When the basicity ranged from 0.4 to 0.8, the calcium-containing compound was dominated by calcium iron silicate. Due to incomplete crystallization, the characteristic peaks of silicate seemed inconspicuous. It was noteworthy that with the basicity increased to 1.0, complex calcium ferrite (SFCA) belonged to  $\text{SiO}_2\text{-Fe}_2\text{O}_3\text{-CaO-Al}_2\text{O}_3$  multivariate system appeared in the XRD spectrum. Compared with calcium iron silicate, SFCA possessed higher crystallinity and intensity [20]. Furthermore, the reducibility of SFCA was close to that of hematite, which made it more suitable as the binding phase of fluxed pellets. Conversely, it was difficult for  $\text{Fe}^{3+}/\text{Fe}^{2+}$  to be reduced in the silicate phase [17,21]. According to the composition of calcium-containing substances, we could divide fluxed pellets into two parts of low-basicity (0.4–1.0) and high-basicity (1.0–1.2) pellets. The calcium-containing phase of low-basicity pellets was mainly composed of calcium-iron silicate, while complex calcium ferrite SFCA appeared in the phase of high-basicity pellets universally. The difference in properties between these two calcium-containing phases was the key to analyzing the consolidation mechanism of fluxed pellets with different basicity.

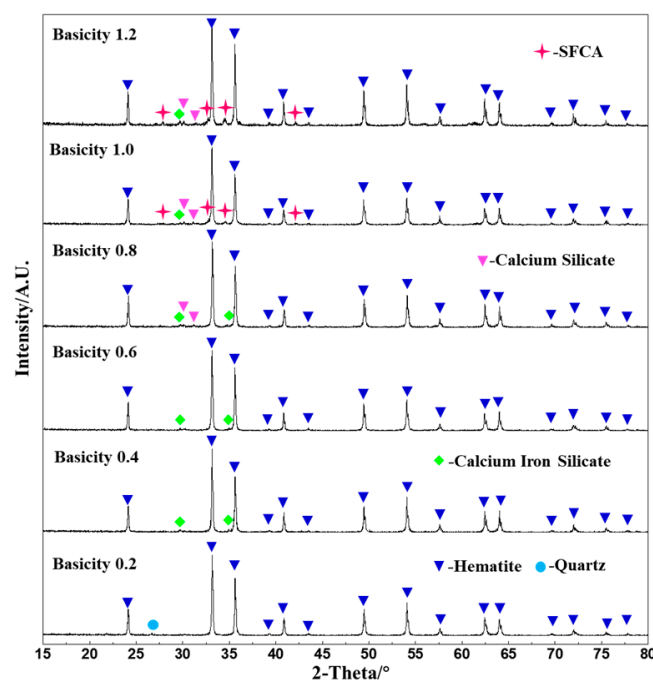


**Figure 5.** XRD patterns of fluxed pellets.

### 3.2. Microstructures Analysis of Different Basicity Fluxed Pellets

#### 3.2.1. Electron Microscope Microstructures of Different Basicity Pellets

To further explore the influence of basicity and calcium-containing substances on the microstructure of fluxed pellets, SEM-EDS analysis was performed on samples with 0.2, 0.4, 0.6 and 1.2 basicity, respectively. As revealed by Figure 6a, the adjacent hematite particles (point 1) formed an interconnected crystal structure by the microcrystalline junction, while the acidic gangue (point 2) existed independently. Consequently, the consolidation method of 0.2 basicity pellets was dominated by the solid-phase consolidation of hematite particles. As the basicity increased to 0.4, low-melting-point calcium-containing compounds that formed during the preheating process would melt into the liquid phase with better fluidity under a high roasting temperature. The liquid phase adhered to hematite grains and brought adjacent particles close to each other by surface tension. After cooling, calcium iron silicate (point 3) was formed to assist the pellets consolidate, which was confirmed by the results in Figure 6b. It was observed that the consolidation of 0.4 basicity pellets depended on both the hematite microcrystalline connection and calcium iron silicate glassy phase bonding. From Figure 6c, when the basicity of the pellets reached 0.6, more calcium iron silicate (point 4) filled between the hematite particles. In the roasting process, small hematite particles could melt into a high-temperature liquid phase, while large hematite particles grew continuously and formed smooth crystalline grains by eliminating lattice defects. As shown in Figure 6d, by further increasing the basicity to 1.2, a large amount of complex calcium ferrite (SFCA) was generated in high-basicity fluxed pellets and replaced calcium iron silicate as the main binding phase to assist consolidation. As previously stated, SFCA could provide higher strength and better reducibility than the calcium iron silicate glassy phase; therefore, high-basicity fluxed pellets exhibited obvious advantages in the microstructure. Figure 6e,f are the 5000 $\times$  magnification backscattering electron (BSE) images of SFCA. Figure 6e shows the section view of SFCA grains, while Figure 6f exhibits the three-dimensional morphology of SFCA grains. The SFCA (Point 5) and calcium silicate (Point 6) were formed by cooling the crystallized calcium-containing molten liquid phase. It was found that the lamellar SFCA crystal formed a more complete crystal morphology than the silicate phase, thus providing higher strength for fluxed pellets. Despite this, there were some obvious pores in the microstructure of high-basicity (1.2) fluxed pellets, which could also have negative effects on the strength.



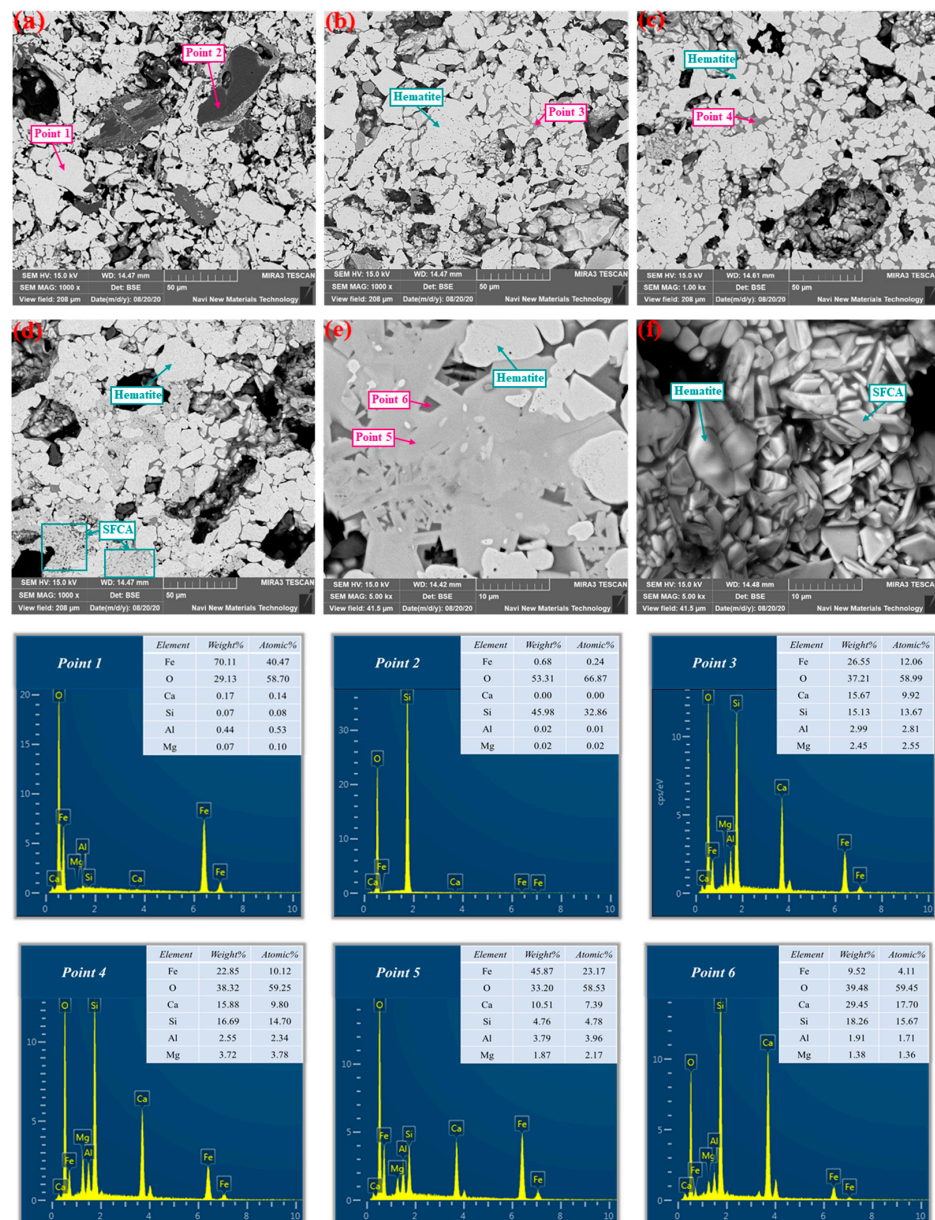


**Figure 6.** SEM-EDS analysis of fluxed pellets ((a) 0.2 basicity, (b) 0.4 basicity, (c) 0.6 basicity, (d) 1.2 basicity, (e) SFCA and calcium silicate and (f) the morphology of SFCA).

### 3.2.2. Element Distribution Analysis of High-Basicity Pellets

As described in the previous investigation, high-basicity (1.0–1.2) fluxed pellets exhibit better strength and reducibility because of the particularity of the calcium-containing binding phase. For this reason, EPMA technology was used to conduct further research on the element distribution and element migration characteristics of high-basicity fluxed pellets to reveal the formation mechanism of the calcium-containing binding phase. According to Figure 7, the distribution of Fe, Ca, Si, Al, Mg and O elements was detected, respectively, in 1.2 basicity pellets. The results showed that Fe was mainly distributed in the hematite particles and, to a lesser extent, in the binding phase. The distribution areas of calcium and silicon were consistent, both aggregated in the binding-phase SFCA and calcium silicate. Impurity elements appeared in SFCA crystal, including aluminum and magnesium, which confirmed that SFCA belonged to the multivariate complex system, unlike the pure substances of calcium ferrite ( $\text{CaFe}_2\text{O}_4$ ) and dicalcium ferrite ( $\text{Ca}_2\text{Fe}_2\text{O}_5$ ). This was because, in the preheating process,  $\text{CaO}$  and  $\text{Fe}_2\text{O}_3$  react to form the calcium ferrite phase. During

the high-temperature ( $>1205\text{ }^{\circ}\text{C}$ ) roasting process, calcium ferrite ( $\text{CaFe}_2\text{O}_4$ ) would first melt into the liquid phase, which promoted  $\text{Al}^{3+}$ ,  $\text{Si}^{4+}$  and  $\text{Mg}^{2+}$  from silicates migrating into the calcium ferrite liquid phase. Finally, the calcium ferrite liquid phase interacted with  $\text{Al}^{3+}$ ,  $\text{Si}^{4+}$  and  $\text{Mg}^{2+}$  to form SFCA as a solid solution [22,23]. Even so, SFCA still maintained excellent physical and metallurgical properties, which could be preferred as the main binding phase of fluxed pellets.

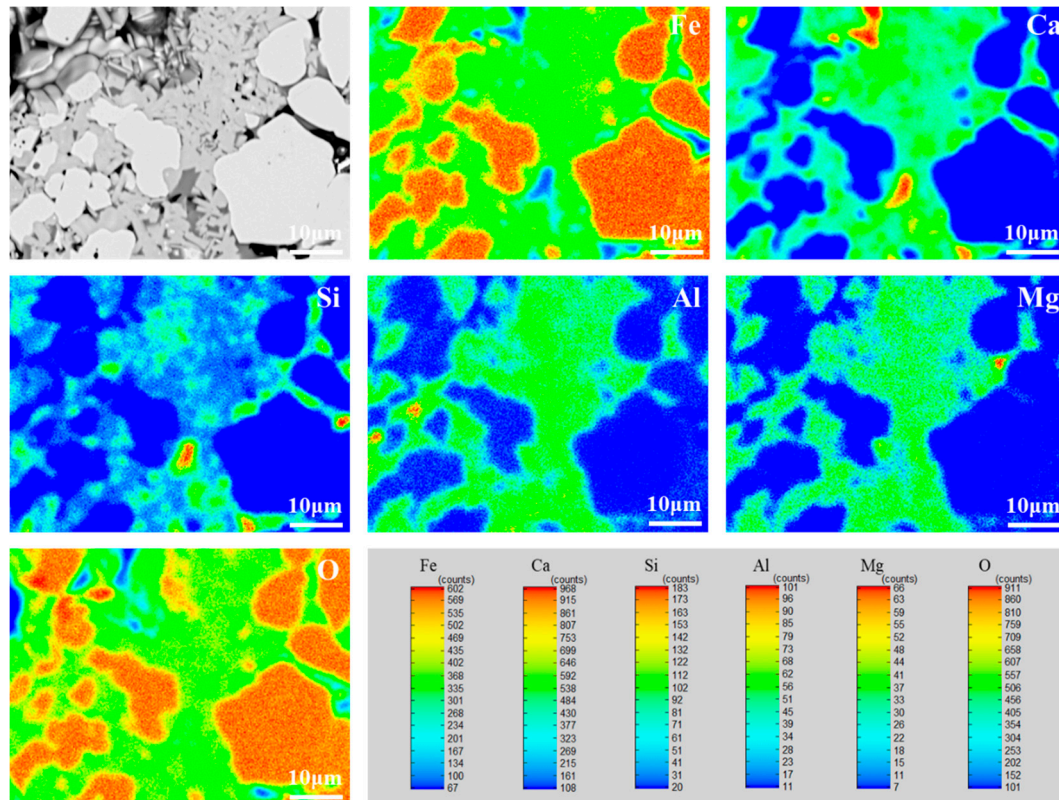


**Figure 7.** EPMA analysis of fluxed pellets with 1.2 basicity.

### 3.2.3. Proportion Variation of Different Microstructures with Basicity

The above studies have confirmed the importance of the calcium-containing binding phase including complex calcium ferrite SFCA and calcium iron silicate for fluxed pellets consolidation. To further investigate the influence of basicity on the calcium-containing binding phase, the optical microscope image analysis technique was used to calculate the hematite, binding phase and pore area proportions in different basicity fluxed pellets. Note that the image analysis technique was unable to accurately quantify the content of the calcium-containing binding phase; however, the statistical results could contribute to finding out the changing trend of its proportion. As revealed in Figure 8, the area percentage of the calcium-containing binding phase rose continuously with the increase in basicity, which was mainly attributed to the fact that the addition of limestone enhanced the formation of calcium iron silicate, calcium silicate and SFCA. When the basicity reached 0.4, the reason for the area percentage decrease in pores was because a small amount of liquid phase produced by the melting of calcium-containing compounds during high-temperature roasting helped repair the defects and promote the densification of the pellets' structure. However, as the basicity continued to rise, the excessive molten liquid would regenerate new pores after cooling and shrinking, which was consistent with the statistical results. When the basicity of fluxed pellets ranged from 1.0 to 1.2, the area percentage of hematite particles decreased significantly, mainly because the formation of SFCA required the participation of  $\text{Fe}_2\text{O}_3$ . In general, the increase in basicity promoted the accumulation



of the calcium-containing binding phase, which could provide more assistance in the consolidation of fluxed pellets.

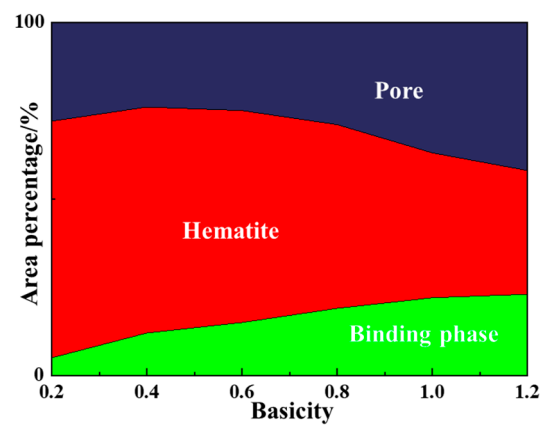


**Figure 8.** The effect of basicity on hematite, binding phase and pore area fractions.

### 3.3. Consolidation Mechanism of Fluxed Pellets

The main consolidation mechanism of different basicity pellets could be divided into three categories, namely, the consolidation dominated by hematite microcrystalline connection and the assistant consolidation of the calcium-containing binding phase, including calcium iron silicate or complex calcium ferrite SFCA. These three consolidation methods corresponded to natural-basicity (0–0.4) pellets, low-basicity (0.4–1.0) fluxed pellets and high-basicity (1.0–1.2) fluxed pellets, respectively. The consolidation mechanism of fluxed pellets with these above basicity ranges is schematically depicted in Figure 9.

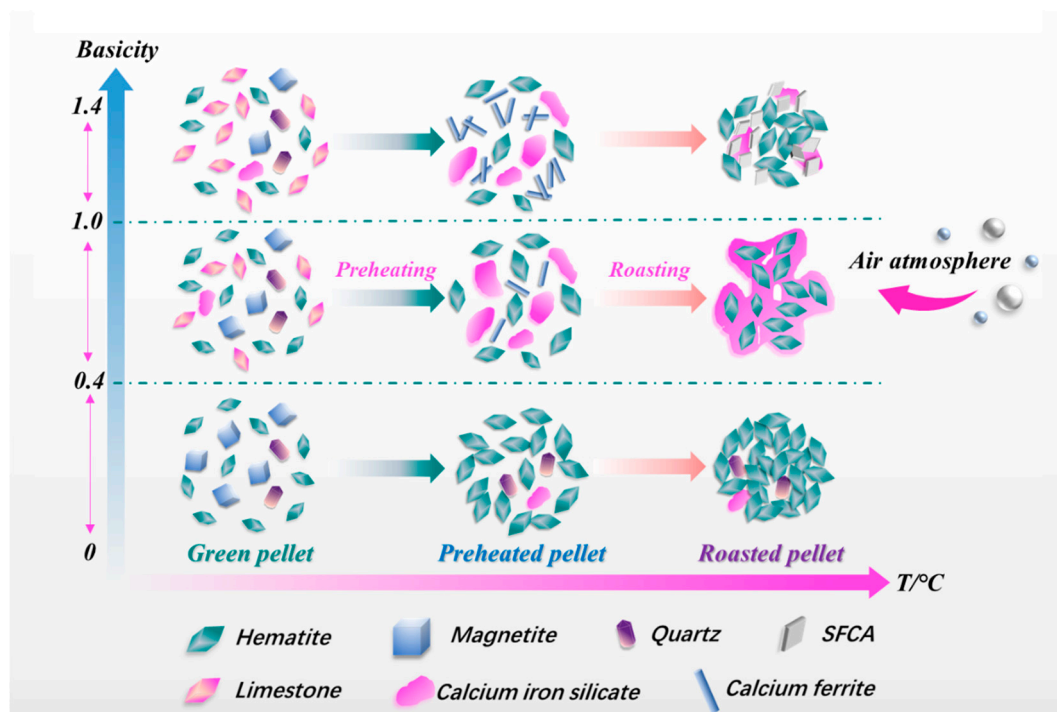


**Figure 9.** Consolidation mechanism model of fluxed pellets.

The hematite crystals in the natural-basicity (0–0.4) green pellets grow continuously during the preheating and roasting process. Meanwhile, the lattice expansion of the newly formed crystal and high ion migration ability on the crystal surface was advantageous for the formation of crystal bridging between adjacent hematite grains. Natural basicity

pellets were finally consolidated by microcrystalline connection, which formed through the particle diffusion of adjacent hematite grains.

The CaO produced by limestone decomposition in the low-basicity (0.4–1.0) green pellets could react with  $\text{Fe}_2\text{O}_3$  to form calcium ferrite and react with  $\text{SiO}_2$  to form silicate during the preheating process [24]. With the increase in roasting temperature, calcium ferrite was preferentially melted. Subsequently, a part of calcium silicate and smaller hematite particles dissolved into the liquid phase. Because of the relatively lower CaO/ $\text{SiO}_2$  ratio (0.4–1.0) in fluxed pellets, the calcium-containing liquid phase mainly formed calcium iron silicate glassy phase after cooling and crystallization, which bonded the surrounding hematite particles to realize the consolidation [25]. In addition to hematite solid-phase consolidation, the bonding effect of calcium iron silicate could further assist in the consolidation of low-basicity fluxed pellets.

As the CaO addition continued to increase, more calcium ferrite would be produced in the preheated pellets with 1.0–1.2 basicity. During the process of high-temperature roasting, excess calcium ferrite and silicate fused to form a high iron and calcium liquid phase. After cooling, the molten liquid phase crystallized in the form of multivariate complex calcium ferrite (SFCA) and calcium silicate, which consolidated the surrounding hematite particles together to enhance the strength of high-basicity fluxed pellets.

### 3.4. Thermal Analysis of Fluxed Pellet Preparation Process

The melting temperature of calcium-containing low-melting-point compounds is important for the consolidation of fluxed pellets. The phase transition temperature of low-melting-point compounds in fluxed pellets could be obtained using TG-DSC synchronous thermal analysis technology. In this section, TG-DSC technology was used to measure the weight and heat flow data change in the pelletizing mixture (basicity 0.6 and 1.2) from 30 °C to 1300 °C.

Figure 10a shows the synchronous thermal analysis curve of the low-basicity (0.6) pelletizing mixture. At 315–388 °C, the oxidation reaction of magnetite ( $\text{Fe}_3\text{O}_4$ ) to isomorphous maghemite ( $\gamma\text{-Fe}_2\text{O}_3$ ) gave off heat and formed exothermic peaks. Subsequently, limestone underwent a violent decomposition reaction to produce CaO and  $\text{CO}_2$  at 701–744 °C, accompanied by obvious weight loss. Note that the phase change endothermic peak of 0.6 basicity pellets appeared within the temperature range of 1225–1243 °C, indicating the initial temperature of the liquid phase formation. In this temperature range, calcium iron silicate from 0.6 basicity pellets gradually melted to form a binding phase to promote the consolidation. Therefore, when preparing 0.6 basicity pellets, the roasting temperature should be controlled above 1225 °C.

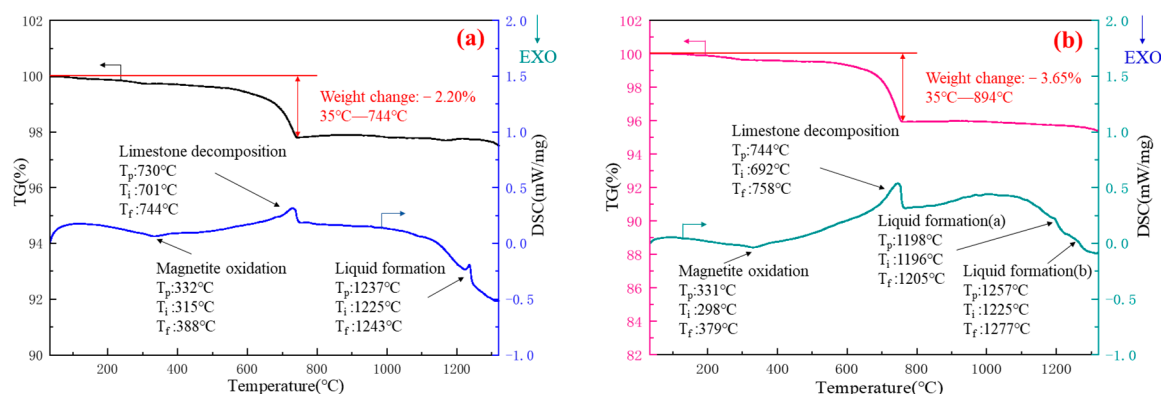


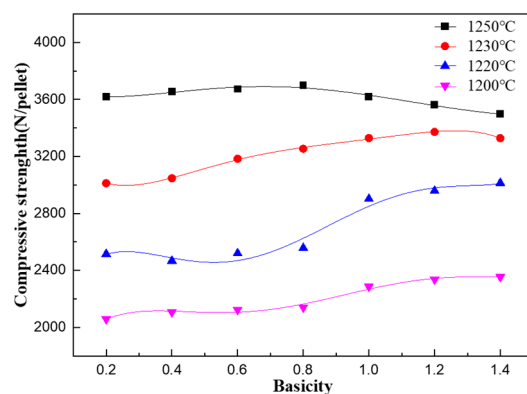
Figure 10. TG/DSC curves of fluxed pellets ((a) 0.6 basicity; (b) 1.2 basicity).

Figure 10b presents the TG-DSC diagram of the high-basicity (1.2) pelletizing mixture. Owing to the increase in limestone addition, the weight loss of the high-basicity pelletizing mixture was even more pronounced. In addition, there were two phase change endothermic peaks on the differential scanning calorimetry curve of the high-basicity (1.2) pelletizing

mixture. The first endothermic peak at 1196–1205 °C was the melting temperature range of the calcium ferrite phase, and the liquid phase generated during this stage could form the binding phase to provide partial strength to the fluxed pellets after cooling. According to the temperature range of the second endothermic peak at 1225–1277 °C, the calcium iron silicate phase in the 1.2 basicity pellets began to melt at 1225 °C, and the liquid phase was generated at this stage would provide additional consolidation strength. To sum up, in order to ensure there was enough liquid phase to promote the consolidation, the roasting temperature of fluxed pellets should be at least higher than 1225 °C.

### 3.5. Influence of Basicity on the Consolidation Strength of Fluxed Pellets

Figure 11 compared the consolidation strength of fluxed pellets with basicity from 0.2–1.4 prepared by different roasting temperatures. When the roasting temperature reached 1200 °C, fluxed pellets with each basicity exhibited lower strength. As the roasting temperature increased to 1220 °C, a small amount of calcium ferrite phase could be melted to assist the consolidation of pellets; hence, fluxed pellets with 1.0–1.4 basicity are more likely to obtain higher strength at this temperature. By comparison, the pellets with 0.2–0.8 basicity formed less binding phase and incomplete hematite microcrystalline connection, which resulted in relatively lower consolidation strength. When the roasting temperature rose to 1230 °C, fluxed pellets exhibited better consolidation strength. This was mainly attributed to the melting of the majority of low-melting-point calcium-containing compounds, which ensured an adequate binding phase for consolidation. At 1250 °C, the microcrystalline connection strength between hematite grains enhanced significantly, which made the compressive strength of natural-basicity pellets (0.2) even stronger than high-basicity (1.0–1.2) fluxed pellets. Furthermore, it was worth noting that when the basicity is above 1.2, excessive liquid phase would be produced to decrease the consolidation strength of fluxed pellets, which was related to the increase in porosity. Taken together, these results suggested that the increase in basicity contributed to the fluxed pellets obtaining better strength within an appropriate range of roasting temperature.



**Figure 11.** The effect of basicity on the compressive strength of fluxed pellets.

## 4. Conclusions

Herein, the influence of basicity and calcium-containing substances on the consolidation mechanism of fluxed pellets was investigated based on the examination results of synchronous thermal analysis, phase composition analysis, microstructure analysis and element distribution analysis. The increase in basicity contributed to promoting the formation of a calcium-containing binding phase, thus providing more assistance for the consolidation of fluxed pellets. Moreover, increasing the roasting temperature appropriately above 1225 °C was helpful in ensuring sufficient binding phase assisted the consolidation of fluxed pellets.

For fluxed pellets, the calcium-containing binding phase could adhere to the surface of hematite grains, bringing adjacent hematite particles close to each other and bonding

together. The type and content of calcium-containing substances in fluxed pellets changed with the basicity. When the basicity ranged from 0.4 to 1.0, calcium iron silicate dominated in the calcium-containing binding phase. As the basicity further increased above 1.0, multivariate complex calcium ferrite (SFCA) with better crystalline and reducibility generated prominently in fluxed pellets. In order to improve the physical and metallurgical properties, the basicity should be increased above 1.0 to prepare fluxed pellets with SFCA as the main calcium-containing binding phase.

**Author Contributions:** Conceptualization, F.C. and Y.G.; methodology, Y.G.; software, S.W.; validation, Y.G.; formal analysis, K.L.; investigation, F.C.; resources, Y.G.; data curation, Y.L.; writing—original draft preparation, K.L.; writing—review and editing, F.C. and Y.G.; visualization, L.Y.; supervision, Y.G.; project administration, Y.G.; funding acquisition, Y.G. All authors have read and agreed to the published version of the manuscript.

**Funding:** This research was funded by the National Natural Science Foundation of China (Grant No. 51904348), Shanxi Province Major Science and Technology projects (Grant No. 20191101002) and the Central South University Post-graduate Independent Exploration and Innovation Projects (2021zzts0294 and 2021zzts0902).

**Data Availability Statement:** Not applicable.

**Conflicts of Interest:** The authors declare no conflict of interest.

## References

1. Dwarapudi, S.; Banerjee, P.; Chaudhary, P.; Sinha, S.; Chakraborty, U.; Sekhar, C.; Venugopalan, T.; Venugopal, R. Effect of fluxing agents on the swelling behavior of hematite pellets. *Int. J. Miner. Process.* **2014**, *126*, 76–89. [\[CrossRef\]](#)
2. Zhou, H.; Zhou, M.; Liu, Z.; Cheng, M.; Chen, J. Modeling NO<sub>x</sub> emission of coke combustion in iron ore sintering process and its experimental validation. *Fuel* **2016**, *179*, 322–331. [\[CrossRef\]](#)
3. Mohanty, M.K.; Mishra, S.; Mishra, B.; Sarkar, S. Effect of Basicity on the Reduction Behavior of Iron Ore Pellets. *Arab. J. Sci. Eng.* **2018**, *43*, 5989–5998. [\[CrossRef\]](#)
4. Wang, R.; Zhang, J.; Liu, Z.; Li, Y. Effect of lime addition on the mineral structure and compressive strength of magnesium containing pellets. *Powder Technol.* **2020**, *376*, 222–228. [\[CrossRef\]](#)
5. Pal, J.; Arunkumar, C.; Rajshekhar, Y.; Das, G.; Goswami, M.C.; Venugopalan, T. Development on Iron Ore Pelletization Using Calcined Lime and MgO Combined Flux Replacing Limestone and Bentonite. *ISIJ Int.* **2014**, *54*, 2169–2178. [\[CrossRef\]](#)
6. Dwarapudi, S.; Ghosh, T.K.; Shankar, A.; Tathavadkar, V.; Bhattacharjee, D.; Venugopal, R. Effect of pellet basicity and MgO content on the quality and microstructure of hematite pellets. *Int. J. Miner. Process.* **2011**, *99*, 43–53. [\[CrossRef\]](#)
7. Prakash, S.; Goswami, M.; Mahapatra, A.; Ghosh, K.; Das, S.; Sinha, A.; Mishra, K. Morphology and reduction kinetics of fluxed iron ore pellets. *Ironmak. Steelmak.* **2000**, *27*, 194–201. [\[CrossRef\]](#)
8. Li, W.; Wang, N.; Fu, G.; Chu, M.; Zhu, M. Influence of roasting characteristics on gas-based direct reduction behavior of Hongge vanadium titanomagnetite pellet with simulated shaft furnace gases. *Powder Technol.* **2017**, *310*, 343–350. [\[CrossRef\]](#)
9. Li, J.; An, H.F.; Liu, W.X.; Yang, A.M.; Chu, M.S. Effect of basicity on metallurgical properties of magnesium fluxed pellets. *J. Iron Steel Res. Int.* **2019**, *27*, 239–247. [\[CrossRef\]](#)
10. Sharma, T.; Gupta, R.; Prakash, B. Effect of gangue content on the swelling behaviour of iron ore pellets. *Miner. Eng.* **1990**, *3*, 509–516. [\[CrossRef\]](#)
11. Iljana, M.; Kemppainen, A.; Paananen, T.; Mattila, O.; Pisilä, E.; Kondrakov, M.; Fabritius, T. Effect of adding limestone on the metallurgical properties of iron ore pellets. *Int. J. Miner. Process.* **2015**, *141*, 34–43. [\[CrossRef\]](#)
12. Panigrahy, S.C.; Jena, B.C.; Rigaud, M. Characterization of bonding and crystalline phases in fluxed pellets using peat moss and bentonite as binders. *Met. Mater. Trans. A* **1990**, *21*, 463–474. [\[CrossRef\]](#)
13. Yang, C.C.; Zhu, D.Q.; Pan, J.; Zhou, B.Z.; Xun, H. Oxidation and Induration Characteristics of Pellets Made from Western Australian Ultrafine Magnetite Concentrates and Its Utilization Strategy. *J. Iron Steel Res. Int.* **2016**, *23*, 924–932. [\[CrossRef\]](#)
14. Gao, Q.J.; Jiang, X.; Wei, G.; Shen, F.M. Effects of MgO on densification and consolidation of oxidized pellets. *J. Cent. South Univ.* **2014**, *21*, 877–883. [\[CrossRef\]](#)
15. Tang, J.; Chu, M.S.; Feng, C.; Li, F.; Liu, Z.G. Phases Transition and Consolidation Mechanism of High Chromium Vanadium-Titanium Magnetite Pellet by Oxidation Process. *High Temp. Mater. Process.* **2015**, *35*, 729–738. [\[CrossRef\]](#)
16. Zhang, F.; Zhu, D.Q.; Pan, J.; Guo, Z.Q.; Xu, M.J. Improving roasting performance and consolidation of pellets made of ultrafine and super-high-grade magnetite concentrates by modifying basicity. *J. Iron Steel Res. Int.* **2020**, *27*, 770–781. [\[CrossRef\]](#)
17. Guo, Y.; Liu, K.; Chen, F.; Wang, S.; Zheng, F.; Yang, L.; Liu, Y. Effect of basicity on the reduction swelling behavior and mechanism of limestone fluxed iron ore pellets. *Powder Technol.* **2021**, *393*, 291–300. [\[CrossRef\]](#)
18. Fan, X.H.; Gan, M.; Jiang, T.; Yuan, L.S.; Chen, X.L. Influence of flux additives on iron ore oxidized pellets. *J. Cent. South Univ. Technol.* **2010**, *17*, 732–737. [\[CrossRef\]](#)



19. Umadevi, T.; Kumar, P.; Lobo, N.F.; Prabhu, M.; Mahapatra, P.; Ranjan, M. Influence of Pellet Basicity (CaO/SiO<sub>2</sub>) on Iron Ore Pellet Properties and Microstructure. *ISIJ Int.* **2011**, *51*, 14–20. [[CrossRef](#)]
20. Nicol, S.; Chen, J.; Pownceby, M.I.; Webster, N.A.S. A Review of the Chemistry, Structure and Formation Conditions of Silico-Ferrite of Calcium and Aluminum (‘SFCA’) Phases. *ISIJ Int.* **2018**, *58*, 2157–2172. [[CrossRef](#)]
21. Cai, B.; Watanabe, T.; Kamijo, C.; Susa, M.; Hayashi, M. Comparison between Reducibilities of Columnar Silico-ferrite of Calcium and Aluminum (SFCA) Covered with Slag and Acicular SFCA with Fine Pores. *ISIJ Int.* **2018**, *58*, 642–651. [[CrossRef](#)]
22. Koryttseva, A.; Webster, N.A.S.; Pownceby, M.; Navrotsky, A. Thermodynamic stability of SFCA (silico-ferrite of calcium and aluminum) and SFCA-I phases. *J. Am. Ceram. Soc.* **2017**, *100*, 3646–3651. [[CrossRef](#)]
23. Zhang, F.; An, S.L.; Luo, G.P.; Wang, Y.C. Effect of Basicity and Alumina-Silica Ratio on Formation of Silico-Ferrite of Calcium and Aluminum. *J. Iron Steel Res. Int.* **2012**, *19*, 1–5. [[CrossRef](#)]
24. Firth, A.R.; Garden, J.F. Interactions between Magnetite Oxidation and Flux Calcination during Iron Ore Pellet Induration. *Met. Mater. Trans. A* **2008**, *39*, 524–533. [[CrossRef](#)]
25. Firth, A.R.; Garden, J.F.; Douglas, J.D. Phase Equilibria and Slag Formation in the Magnetite Core of Fluxed Iron Ore Pellets. *ISIJ Int.* **2008**, *48*, 1485–1492. [[CrossRef](#)]